x-dependence reconstruction of pion and kaon PDFs from Mellin moments author

Constantia Alexandrou,^{a,b} **Simone Bacchio,**^{b} **Ian Cloët,**^{c} **Martha Constantinou,**^{d}
Kyriakos Hadjiyiannakou,^{a,b} **Giannis Koutsou**^{b} **and Colin Lauer**^{c,*}

^{a}*Department of Physics, University of Cyprus, P.O. Box 20537, 1678 Nicosia, Cyprus*

^{b}*Computation-based Science and Technology Research Center, The Cyprus Institute, 20 Kavafi Str., Nicosia 2121, Cyprus*

^{c}*Physics Division, Argonne National Laboratory, Lemont, Illinois 60439, USA*

^{d}*Department of Physics, Temple University, 1925 N. 12th Street, Philadelphia, PA 19122-1801, USA*

E-mail: colin.j.lauer@temple.edu

We present a calculation of the connected-diagram contributions to the first three non-trivial Mellin moments for the pion and kaon, extracted using local operators with up to 3 covariant derivatives. We use one ensemble of gauge configurations with two degenerate light, a strange and a charm quark (N_f =2+1+1) of maximally twisted mass fermions with clover improvement. The ensemble has a pion mass ~260 MeV, and a kaon mass ~530 MeV. We reconstruct the x-dependence of the PDFs via fits to our results, and find that our lattice data favor a $(1-x)^2$-behavior in the large-x region for both the pion and kaon PDFs. We integrate the reconstructed PDFs to extract the higher moments, $\langle x^n \rangle$, with $4 \leq n \leq 6$. Finally, we compare the pion and kaon PDFs, as well as the ratios of their Mellin moments, to address the effect of SU(3) flavor symmetry breaking.

---

*Speaker

1. Introduction

Pion, kaons, and their structures are interesting topics of study in particle physics. Since pions and kaons are both pseudoscalar particles and have similar valence quark structures—the kaon has one light and one strange valence quark instead of two light quarks—comparing their structures can give insights into relations between strong interactions and quark mass effects [1], as well as SU(3) flavor symmetry breaking effects which are caused by the heavier strange quark compared to light quarks [2]. There is some existing experimental data from pion induced Drell-Yan [3], but kaon data is more limited and cannot make definite conclusions about SU(3) symmetry breaking effects. The x-dependence of PDFs has been calculated using Lattice Quantum Chromodynamics (LQCD) (see, e.g. the reviews of Refs. [4–6]), but pions and kaons have not been as studied extensively as the nucleons.

In these proceedings, we use Mellin moments of PDFs to reconstruct the full x-dependence of the pion and kaon PDFs. Reconstructing PDFs from their Mellin moments calculated on the lattice has often been argued to be challenging and even unfeasible. Higher moments include higher uncertainties due to derivatives in the local operators, which introduce more gauge noise, as well as increased noise due to the need for nonzero momentum frames. Additionally, mixing among lower dimensional operators under renormalization is unavoidable when calculating moments higher than $\langle x^3 \rangle$. The combination of these challenges has caused early attempts at reconstructing PDFs [7, 8] to be unable to conclusively determine its feasibility.

Even though these challenges exist, there have been advancements made to computers, algorithms, and computational methods so that Mellin moments of PDFs can be calculated more precisely. In Refs. [9, 10], we calculated the first three nontrivial Mellin moments of the pion and kaon PDFs with the excited state effects reliably removed and without mixing with lower dimensional operators. These improvements motivate us to attempt to reconstruct the x-dependence of the PDFs with three goals: **a.** test the feasibility and limitations reconstructing the PDFs, **b.** observe the behavior of the reconstructed PDFs at large-x, and **c.** use the reconstructed PDFs to calculate the higher moments with $n > 3$.

2. Theoretical and Lattice Setup

For our calculations we use a gauge ensemble produced by the Extended Twisted Mass Collaboration (ETMC) [11]. The ensemble, labeled cA211.30.32, uses $N_f = 2 + 1 + 1$ twisted clover fermions with clover improvement and the Iwasaki improved gluon action. Table 1 contains the key ensemble parameters. The statistics used in the Mellin moment calculations are given in Table 2.

Parameters							
Ensemble	β	a [fm]	volume $L^3 \times T$	N_f	m_π [MeV]	Lm_π	L [fm]
cA211.30.32	1.726	0.093	$32^3 \times 64$	u, d, s, c	260	4	3.0

Table 1: Parameters of the ensemble used in this study.

Statistics				
t_s/a	# configurations	# source positions	# momentum boost	Total
$\langle x \rangle$ two-point correlators				
—	122	16	1	1,952
$\langle x \rangle$ three-point correlators				
12, 14, 16, 18, 20, 24	122	16	1	1,952
$\langle x^2 \rangle$ & $\langle x^3 \rangle$ two-point correlators				
—	122	72	8	70,272
$\langle x^2 \rangle$ & $\langle x^3 \rangle$ three-point correlators				
12	122	16	8	15,616
14, 16, 18	122	72	8	70,272

Table 2: Statistics used in the Mellin moment calculations.

We calculate the moments at various values of the source-sink separation t_s and perform a two-state fit in order to control excited-state contamination. Refs. [9, 10] contain a full description of the process we use to calculate the PDF moments. In our reconstruction of the pion and kaon PDFs, we use the first three non-trivial Mellin moments using the two-state fit results, which we summarize in Table 3.

method	$\langle x \rangle_{u^+}^{\pi}$	$\langle x \rangle_{u}^{k}$	$\langle x \rangle_{s}^{k}$
2-state	0.261(3)	0.246(2)	0.317(2)

method	$\langle x^2 \rangle_{u^+}^{\pi}$	$\langle x^2 \rangle_{u}^{k}$	$\langle x^2 \rangle_{s}^{k}$	$\langle x^3 \rangle_{u^+}^{\pi}$	$\langle x^3 \rangle_{u}^{k}$	$\langle x^3 \rangle_{s}^{k}$
2-state	0.110(7)	0.096(2)	0.139(2)	0.024(18)	0.033(6)	0.073(5)

Table 3: Final results for the first three non-trivial pion and kaon Mellin moments obtained from the one- and two-state fits.

3. Reconstruction of PDFs

We start the reconstruction of the x-dependent PDFs, $q_M^f(x)$, with the standard functional form

$$q_M^f(x) = N x^{\alpha} (1-x)^{\beta} (1 + \rho \sqrt{x} + \gamma x) , \tag{1}$$

where $(M, f) = (\pi, u), (K, u), (K, s)$. N is a normalization defined by charge conservation, which leads to

$$N = \frac{1}{B(\alpha + 1, \beta + 1) + \gamma B(2 + \alpha, \beta + 1)} , \tag{2}$$

where B is the Euler beta-function. The fit parameters in Eq. (1) are α, β, γ and ρ. We set the parameter ρ to be zero, since it is generally assumed to be negligible [12]. The nth-moment is calculated by taking the integral of Eq. (1), i.e.,

$$\langle x^n \rangle = N \int_0^1 dx\, x^\alpha (1-x)^\beta (1 + \gamma x)\,, \tag{3}$$

which results in

$$\langle x^n \rangle = \frac{\left(\prod_{i=1}^{n}(i+\alpha) \right) \left(n + 2 + \alpha + \beta + (i+1+\alpha)\gamma \right)}{\left(\prod_{i=1}^{n}(i+2+\alpha+\beta) \right) \left(2 + \alpha + \beta + (1+\alpha)\gamma \right)}\,, \quad n > 0\,. \tag{4}$$

We calculate the fit parameters in Eq. (4), using our Mellin moment results given in Table 3 as inputs. We use NNLO expressions to evolve our Mellin moment results to a scale of 5.2 GeV so that comparison can be made to results from global fits and models.

We first test how the reconstructed PDF depends on the number of fit parameters by performing a 2-parameter ($\gamma = 0$) and a 3-parameter fit. We find that the reconstructed PDF are compatible for the two kind of fits, and choose the 2-parameter fit as final method. The obtained fit parameters are given in Table 4. The fits for the pion are less stable than those for the kaon in both cases because the gauge noise is larger in the pion.

type	α	β
π^u	-0.05(19)	2.20(64)
K^u	-0.005(81)	2.59(28)
K^s	0.26(9)	2.27(22)

Table 4: The fit parameters for q_π^u, q_K^u and q_K^s at 5.2 GeV. The error in the parenthesis is statistical.

Using Eq. (1) we reconstruct the x-dependent PDFs and study the effects of excited-states contamination on $q_M^f(x)$. Such effects may be non-trivial due to the moments having a non-linear dependence on the fit parameters in Eq. (1). We perform a 2-parameter fit on our Mellin moment results at $t_s/a = 14 - 18$, as well as the two-state fit and reconstruct the PDFs, as shown in Fig. 1. We find that the PDFs increase with lower t_s, meaning that the excited-state contamination leads to a higher PDF. We see a nice convergence as t_s increases with the two-state fit values eventually converging with a peak around $x \sim 0.3 - 0.4$, i.e., $xq_\pi^u(0.3) \sim 0.4$, $xq_K^u(0.3) \sim 0.4$ and $xq_K^s(0.4) \sim 0.5$. We use the PDFs extracted form the two-state fit results for the moments (purple band in Fig. 1) as our final results.

Since we reconstruct the PDFs using only the $n \leq 3$ moments, we test whether three moments are enough to successfully calculate the x-dependence. To do this, we use the PDF and its moments calculated by the Jefferson Lab Angular Momentum (JAM) collaboration [13]. We use the same procedure as we did previously with our lattice data to reconstruct the JAM PDF, now using as inputs the JAM moments with $n \leq 3$. In Fig. 2, the reconstructed PDF and original JAM PDFs are compared to each other. We find that the two agree well for almost all regions of x within
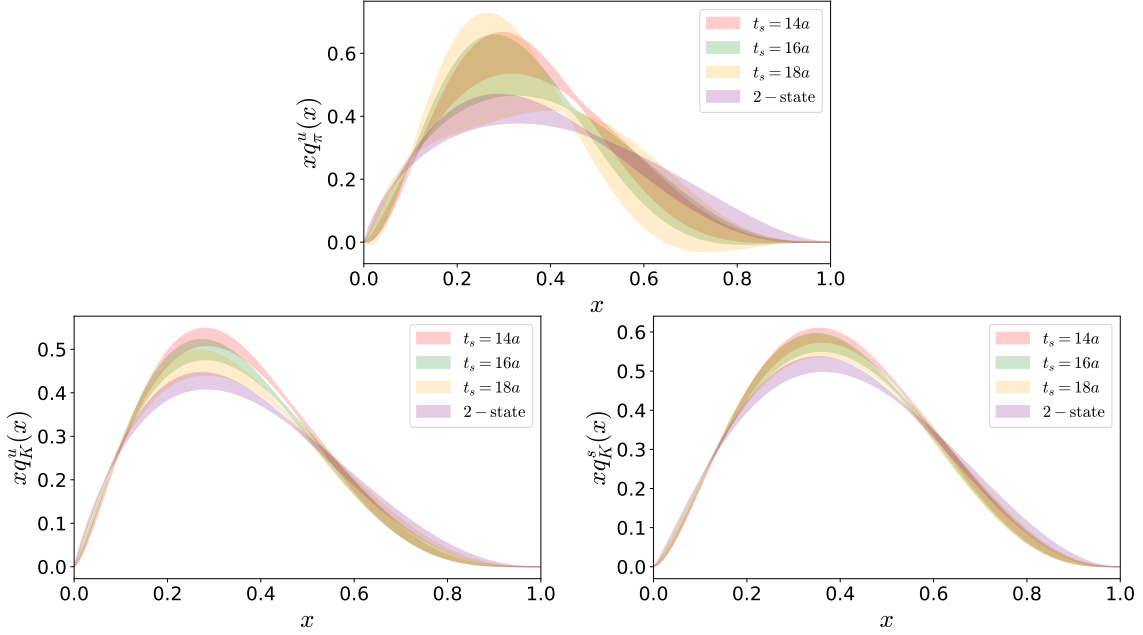
4

Figure 1: The x dependence of $xq_\pi^u(x)$ (top), $xq_K^u(x)$ (lower left panel), and $xq_K^s(x)$ (lower right panel) with t_s/a =14, 16, 18, and the 2-state fit shown as the pink, green, yellow and purple bands, respectively. The results are given in the $\overline{\text{MS}}$ scheme at a scale of 27 GeV^2.

uncertainties. The reconstructed PDF has much larger uncertainties, due to the lost information from truncating the moments at $n = 3$. As another check, we calculate the $n = 4$ moment using the fitting parameters and Eq. (4). We find $\langle x^4 \rangle_\pi^u = 0.026(2)$, which is in excellent agreement with the moment calculated using the JAM framework, $\langle x^4 \rangle_\pi^u = 0.027(2)$ supporting the fact that the PDFs can feasibly be reconstructed using the $n \leq 3$ moments.
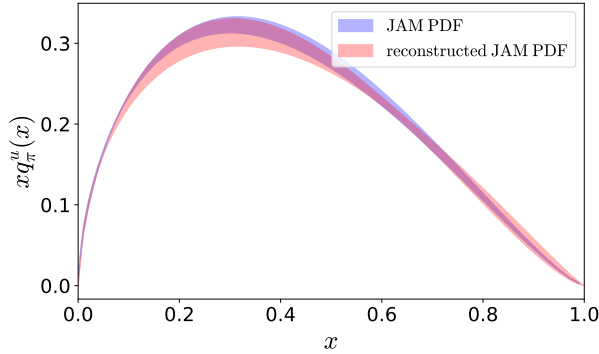
Figure 2: Pion PDF as calculated by the JAM collaboration (blue band) and the PDF reconstructed from its moments with $n \leq 3$ (pink band). The reported scale is 27 GeV^2.

We further test the feasibility of reconstructing the PDFs by performing fits including moments up to $\langle x^{n_{\max}} \rangle$, with $n_{\max} = 2$, 3, or 4. We only use lattice data for $n_{\max} = 2$ and 3, and add another constraint for $n_{\max} = 4$ by using the value of $\langle x^4 \rangle$ obtained from global fits and models for the pion and kaon, respectively. For the pion, we use $\langle x^4 \rangle_\pi^u = 0.027(2)$ from the JAM analysis [13], and

$\langle x^4 \rangle^s_K = 0.029^{+0.005}_{-0.004}$, $\langle x^4 \rangle^u_K = 0.021^{+0.003}_{-0.003}$ from BLFQ-NJL [14] for the kaon. We compare the PDFs reconstructed with $n_{\max}$ = 2, 3, and 4 in Fig. 3. The constraint of the PDFs is improved with the addition of $n = 3$ and, interestingly, the shape of the PDFs are not affected by the addition of $n = 4$. Therefore, the effect of including higher moments in the fits is within the shown uncertainties and we use as our final estimates $n_{\max} = 3$. To summarize our final estimates, we choose the PDFs reconstructed from a 2-parameter fit with our two-state fit lattice results up to $\langle x^3 \rangle$ as inputs.
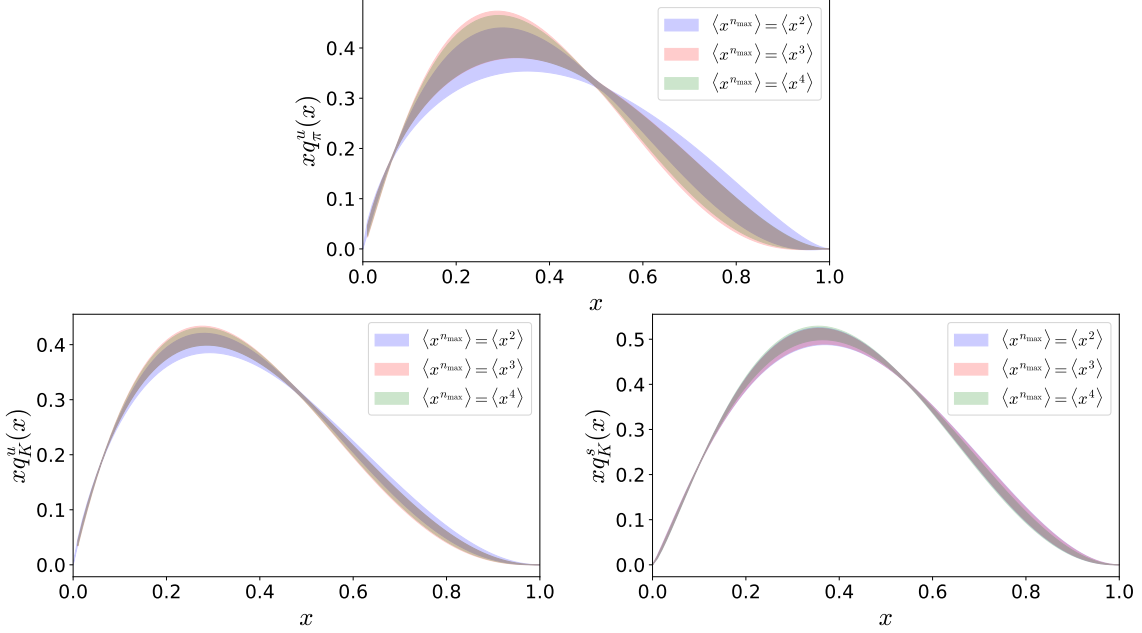
Figure 3: Top: The x dependence of $xq^u_\pi(x)$ using the 2-parameter fit with $\langle x^n_{\max} \rangle = \langle x^2 \rangle$, $\langle x^3 \rangle$, $\langle x^4 \rangle$ The blue, pink and green bands represent $n_{\max} = 2$, 3, and 4, respectively. For the green band, we use $\langle x^4 \rangle^u_\pi$ [13] as a constraint. Bottom: Same as top panel for $xq^u_K(x)$ (left panel) and $xq^s_K(x)$ (right panel) using the BLFQ-NJL [14] $\langle x^4 \rangle_K$ values as constraints for the green band.

The SU(3) flavor symmetry breaking can be studied by comparing pion and kaon PDFs, which we show in Fig. 4. The distributions of the up quarks in both mesons, $xq^u_\pi(x)$ and $xq^u_K(x)$, show a small difference around $x = 0.5$ but are otherwise in full agreement for all regions of x. This behavior suggests that the up quark is equally prevalent in mesons PDFs and is mostly found in the small- to intermediate-x regions. The strange quark is more prevalent in the kaon than the up quark between $x = 0.3$ and $x = 0.8$ and has more support in the large-x region. This is what is expected intuitively given the larger strange quark mass. We find the distribution peaks to be $xq^u_\pi(x = 0.30) = 0.42(5)$, $xq^u_K(x = 0.27) = 0.43(2)$, and $xq^s_K(x = 0.35) = 0.52(2)$.

Once the parameters in Table 4 have been calculated, the Mellin moments can be extracted from Eq. (4). This method of calculating $\langle x^N \rangle$ does not have the problem of operator mixing, which is unavoidable when calculating the moments directly from matrix elements using n^{th}-derivative operators for $n > 3$. Table 5 shows the moments for $n \le 6$ calculated from the parameters in Table 4 calculated using the 2-parameter fit. The first parenthesis are the statistical and the second are the excited state systematic errors, which are calculated as the difference between the mean moments
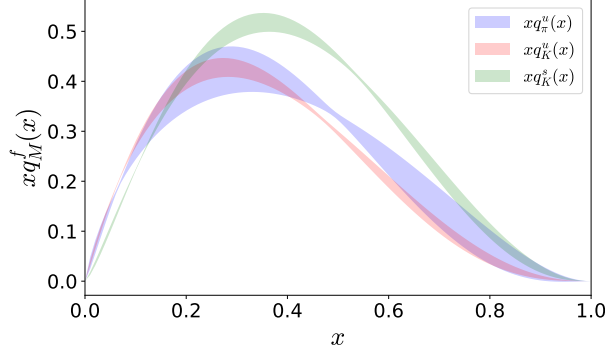
Figure 4: Comparison of $xq_\pi^u(x)$ (blue band), $xq_K^u(x)$ (pink band) and $xq_K^s(x)$ (green band) at 27 GeV^2. The PDFs are reconstructed using our lattice data up to $\langle x^3 \rangle$ and with the 2-state fits analysis and a 2-parameter fit.

calculated from the two-state fit and the plateau fit at the largest source-sink separation. We find that our uncertainties are well behaved, even for $n > 3$.

q_M^f	$\langle x \rangle$	$\langle x^2 \rangle$	$\langle x^3 \rangle$
q_π^u	0.229(3)(7)	0.087(5)(7)	0.042(5)(9)
q_K^u	0.217(2)(5)	0.077(2)(1)	0.035(2)(2)
q_K^s	0.279(1)(5)	0.114(2)(4)	0.057(2)(2)
q_M^f	$\langle x^4 \rangle$	$\langle x^5 \rangle$	$\langle x^6 \rangle$
q_π^u	0.023(5)(7)	0.014(4)(6)	0.009(3)(4)
q_K^u	0.019(1)(2)	0.011(1)(1)	0.007(1)(1)
q_K^s	0.032(2)(2)	0.020(1)(2)	0.013(1)(2)

Table 5: The first six pion and kaon Mellin moments in $\overline{\text{MS}}$ at 27 GeV^2 as calculated from α and β in Table 1 and Eq. (4). The first parenthesis contain the statistical error and the second parenthesis contain the systematic error caused by excited-states contamination.

3.1 Comparison with other studies

In Fig. 5 we compare our results to some of the other existing calculations of the pion and kaon PDFs. In the left upper panel, our results are compared to lattice results of PDFs calculated with the pseudo-ITD approach [15] and the current-current correlators (LCS) method [16, 17]. We find that our results agree better with the LCS method, while the peak from pseudo-ITD study is lower than ours. Our results are also compared to the E615 [3], and ASV PDFs [18], and the JAM Collaboration's global fits [13, 19]. In the upper right panel, our results are compared with PDFs calculated using Dyson-Schwinger equations (DSE) [12], the updated DSE '18 [20], the chiral constituent quark model (χCQ) [21], the BLFQ Collaboration [14] PDFs calculated using light front quantization and QCD evolution (NJL). Calculations of the kaon PDFs are more limited. In the lower panels of Fig. 5, our results for the up quark (left) and strange quark (right) are compared

with the χCQ [21], BLFQ-NJL [14], and DSE '18 [20] results. We find good agreement between all of the studies for the pion and $xq_K^u(x)$ in the small-x region ($x < 0.1$), although the slope of χCQ at small-x is different from the others. Except for E615, our results are in agreement with the other studies for $x > 0.6$. Most of the tension between studies exists in the intermediate region. For the pion, our results are in agreement with DSE [12] for all regions of x, but we calculate a higher peak than DSE'18. In the small- and large-x regions of the kaon, the PDFs agree qualitatively, while in the intermediate-x region, our results are larger than the other results. The kaon comparisons, however, are only qualitative, since no experimental data exist and non-quantified systematic uncertainties are present in all of the calculations.

The large-x behavior of the pion and kaon PDFs is an interesting topic of study because different analyses of experimental data and model calculations have found different large-x behavior. For instance, one analysis of the pion Drell-Yan data from the Fermilab E615 experiment [3] finds that the PDF falls at large-x like $(1-x)^1$ which corresponds to $\beta = 1$, while a more recent analysis [18] suggests the fall to go like $(1-x)^2$ ($\beta = 2$). The study using DSE [12] also calculates β to be closer to 2. Lattice QCD offers a desirable alternative to address this tension. In this work, we find a value for β around 2, shown in Table 4. Based on these values, we find that both the pion and kaon PDFs drop off like $\sim (1-x)^2$ at large-x.
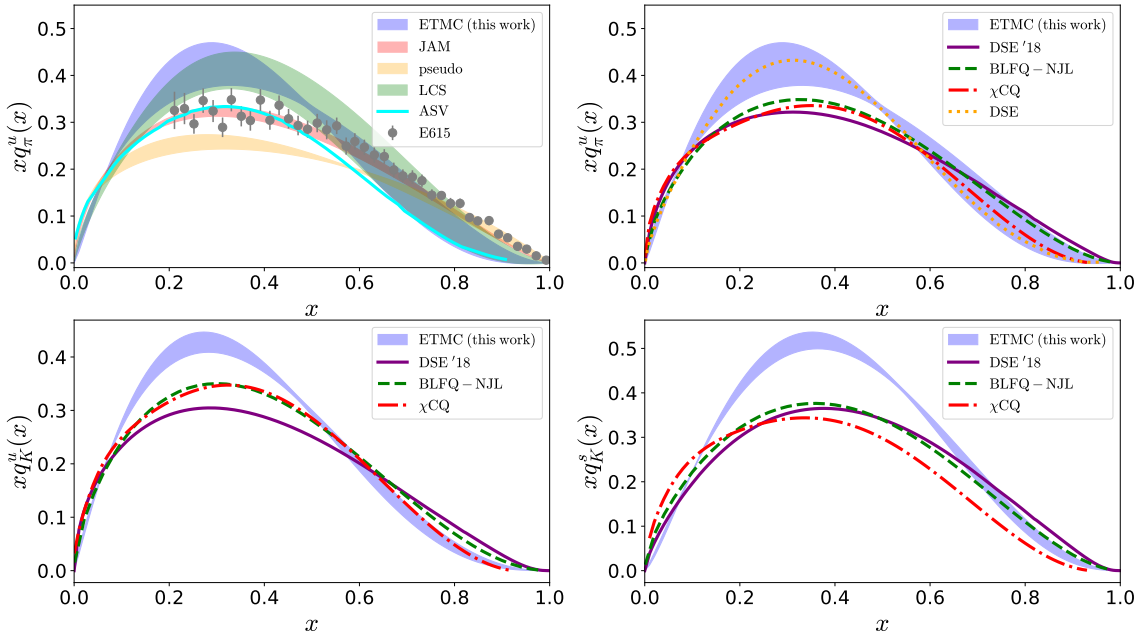

Figure 5: Top left panel: Comparison between our results for the pion $xq_\pi^u(x)$ and other studies, all in the $\overline{\mathrm{MS}}$ scheme at 27 GeV^2. Our results are plotted as the blue band, the E615 data [3] as the gray points, the rescaled ASV curve [18] as the cyan line, the JAM global fit as the pink band, the pseudo-ITD [15] lattice results as the orange band, and the current current correlators (LCS) lattice results [17] as the green band. Top right panel: Comparison between our results for $xq_\pi^u(x)$, DSE [12] (orange dotted line), the updated DSE'18 [20] (purple solid line), BLFQ-NJL [14] (green dashed line), and χCQ [21] (red dot-dashed line). Bottom panel: Same as top panel for the kaon $xq_K^u(x)$ (left) and $xq_K^s(x)$ (right).

4. Summary

We use the pion and kaon Mellin moments up to $\langle x^3 \rangle$ to reconstruct the x-dependence of the PDFs. We fit the moments to the standard functional form for PDFs, using 2-parameter and 3-parameter fits and find the 2-parameter fit to be sufficient to reconstruct the PDFs. We study excited-states effects and find non-negligible excited-states contamination for source-sink time separations below 1.5 fm, requiring the use of a two-state fit to control systematic uncertainties. We also test the dependence on the moments included in the fit by reconstructing the PDFs with the highest moment included to be $\langle x^2 \rangle$, $\langle x^3 \rangle$, or $\langle x^4 \rangle$. Our results suggest that the PDF reconstruction is not improved by including $\langle x^4 \rangle$.

We use our PDF results to study pion and kaon structure in multiple ways. The first is the large-x behavior of the PDFs which we find to be $\sim (1-x)^2$. The second is to calculate the higher moments using the fitting parameters and integrals of the functional form of the PDFs. We show results up to $\langle x^6 \rangle$. Lastly, we study the SU(3) flavor symmetry breaking by comparing the pion PDF to the two quark flavor PDFs of the kaon. We find that the distributions of the light quarks are approximately the same in the pion and kaon and that the strange quark distribution in the kaon is larger in the intermediate- to large-x region.

Acknowledgments

References

[1] P.T.P. Hutauruk, I.C. Cloet and A.W. Thomas, *Flavor dependence of the pion and kaon form factors and parton distribution functions*, *Phys. Rev. C* **94** (2016) 035201 [1604.02853].

[2] Particle Data Group collaboration, *Review of Particle Physics*, *PTEP* **2020** (2020) 083C01.

[3] J.S. Conway et al., *Experimental Study of Muon Pairs Produced by 252-GeV Pions on Tungsten*, *Phys. Rev.* **D39** (1989) 92.

[4] K. Cichy and M. Constantinou, *A guide to light-cone PDFs from Lattice QCD: an overview of approaches, techniques and results*, *accepted in Advances of High Energy Physics* (2018) [1811.07248].

[5] M. Constantinou, *The x-dependence of hadronic parton distributions: A review on the progress of lattice QCD*, *Eur. Phys. J. A* **57** (2021) 77 [2010.02445].

[6] K. Cichy, *Progress in x-dependent partonic distributions from lattice QCD*, in *38th International Symposium on Lattice Field Theory*, 10, 2021 [2110.07440].

[7] W. Detmold, W. Melnitchouk and A.W. Thomas, *Parton distributions from lattice QCD*, *Eur. Phys. J. direct* **3** (2001) 13 [hep-lat/0108002].

[8] R.J. Holt and C.D. Roberts, *Nucleon and pion distribution functions in the valence region*, *Reviews of Modern Physics* **82** (2010) 2991–3044.

[9] ETM collaboration, *Mellin moments $\langle x \rangle$ and $\langle x^2 \rangle$ for the pion and kaon from lattice QCD*, *Phys. Rev. D* **103** (2021) 014508 [2010.03495].

[10] ETM COLLABORATION collaboration, *Pion and kaon $<x^3>$ from lattice qcd and pdf reconstruction from mellin moments*, *Phys. Rev. D* **104** (2021) 054504 [2104.02247].

[11] C. Alexandrou et al., *Simulating twisted mass fermions at physical light, strange and charm quark masses*, *Phys. Rev.* **D98** (2018) 054518 [1807.00495].

[12] C. Chen, L. Chang, C.D. Roberts, S. Wan and H.-S. Zong, *Valence-quark distribution functions in the kaon and pion*, *Phys. Rev. D* **93** (2016) 074021 [1602.01502].

[13] P. Barry, N. Sato, W. Melnitchouk and C.-R. Ji, *First Monte Carlo Global QCD Analysis of Pion Parton Distributions*, *Phys. Rev. Lett.* **121** (2018) 152001 [1804.01965].

[14] J. Lan, C. Mondal, S. Jia, X. Zhao and J.P. Vary, *Pion and kaon parton distribution functions from basis light front quantization and QCD evolution*, *Phys. Rev. D* **101** (2020) 034024 [1907.01509].

[15] B. Joó, J. Karpie, K. Orginos, A.V. Radyushkin, D.G. Richards, R.S. Sufian et al., *Pion Valence Structure from Ioffe Time Pseudo-Distributions*, *Phys. Rev.* **D100** (2019) 114512 [1909.08517].

[16] R.S. Sufian, J. Karpie, C. Egerer, K. Orginos, J.-W. Qiu and D.G. Richards, *Pion Valence Quark Distribution from Matrix Element Calculated in Lattice QCD*, *Phys. Rev.* **D99** (2019) 074507 [1901.03921].

[17] R.S. Sufian, C. Egerer, J. Karpie, R.G. Edwards, B. Joó, Y.-Q. Ma et al., *Pion Valence Quark Distribution from Current-Current Correlation in Lattice QCD*, *Phys. Rev. D* **102** (2020) 054508 [2001.04960].

[18] M. Aicher, A. Schafer and W. Vogelsang, *Soft-gluon resummation and the valence parton distribution function of the pion*, *Phys. Rev. Lett.* **105** (2010) 252003 [1009.2481].

[19] N.Y. Cao, P.C. Barry, N. Sato and W. Melnitchouk, *Towards the 3-dimensional parton structure of the pion: integrating transverse momentum data into global qcd analysis*, 2021.

[20] K.D. Bednar, I.C. Cloët and P.C. Tandy, *Distinguishing Quarks and Gluons in Pion and Kaon Parton Distribution Functions*, *Phys. Rev. Lett.* **124** (2020) 042002 [1811.12310].

[21] A. Watanabe, T. Sawada and C.W. Kao, *Kaon quark distribution functions in the chiral constituent quark model*, *Phys. Rev. D* **97** (2018) 074015 [1710.09529].